




Article

# Ultrasound Findings of Monosodium Urate Aggregates in Patients with Gout

Eric Liu <sup>1,\*</sup>, Nicola Dalbeth <sup>2</sup>, Bregina Pool <sup>2</sup>, Andrea Ramirez Cazares <sup>3</sup>, Veena K. Ranganath <sup>1</sup>  
and John D. FitzGerald <sup>1,4</sup> 

<sup>1</sup> Department of Medicine, David Geffen School of Medicine, University of California, Los Angeles, CA 90095, USA

<sup>2</sup> Department of Medicine, University of Auckland, Auckland 1023, New Zealand

<sup>3</sup> Touro College of Osteopathic Medicine, Touro University, New York, NY 10027, USA

<sup>4</sup> Department of Medicine, Veteran Affairs Administration, Los Angeles, CA 90073, USA

\* Correspondence: ericliu@mednet.ucla.edu

**Abstract:** Aggregates are one of the elementary lesions seen on musculoskeletal ultrasound (US) in gout patients as defined by Outcome Measures in Rheumatology (OMERACT). The aim of this study was to evaluate the threshold of detection of aggregate findings on ultrasound and to analyze these findings with corresponding compensated light microscope (CPLM) images in vitro. Patient derived monosodium urate (MSU) crystals were obtained from two separate patients with gout during routine clinical care. In addition, fabricated in-house synthetic MSU crystals were used for comparison. Each sample was scanned using a GE Logic ultrasound machine and corresponding CPLM images obtained. As the aggregates became imperceptible by ultrasound, MSU clumping by CPLM examination was no longer detectable and crystal density per high power field fell markedly. Aggregates on US images are present only from patient-derived samples likely representing MSU crystal clustering or packing. Thus, when synovial aspiration is considered, a joint with aggregates on US would be a more suitable target with a higher likelihood of noting MSU crystals.

**Keywords:** musculoskeletal ultrasound; aggregates; gout; monosodium urate crystals; CPLM



**Citation:** Liu, E.; Dalbeth, N.; Pool, B.; Ramirez Cazares, A.; Ranganath, V.K.; FitzGerald, J.D. Ultrasound Findings of Monosodium Urate Aggregates in Patients with Gout. *Gout Urate Cryst. Depos. Dis.* **2023**, *1*, 83–88. <https://doi.org/10.3390/gucdd1020008>

Academic Editor: Tristan Pascart

Received: 22 November 2022

Revised: 17 March 2023

Accepted: 4 April 2023

Published: 14 April 2023



**Copyright:** © 2023 by the authors. Licensee MDPI, Basel, Switzerland. This article is an open access article distributed under the terms and conditions of the Creative Commons Attribution (CC BY) license (<https://creativecommons.org/licenses/by/4.0/>).

## 1. Introduction

Gout is the most common form of inflammatory arthritis affecting 8.3 million (3.9%) adults in the United States [1]. The gold standard method to diagnose gout remains joint aspiration and compensated polarized light microscopic (CPLM) analysis of synovial fluid for the presence of monosodium urate (MSU) crystals [2]. Furthermore, microscopic confirmation of MSU crystals is a sufficient criterion per the 2015 ACR/EULAR gout classification criteria [3].

In 2015, the Outcome Measures in Rheumatology (OMERACT) gout ultrasound task force developed consensus-based definitions for ultrasound (US) findings in gout. The elementary lesions in gout were identified as double contour sign (DCS), tophi, erosions, and aggregates [4]. OMERACT defined aggregates as “heterogeneous hyperechoic foci that maintain their high degree of reflectivity, even when the gain setting is minimized or the insonation angle is changed and which occasionally may generate posterior acoustic shadow” [3,5]. The complexity of this definition has created some uncertainty amongst sonographers [6]. Though the exact etiology of these aggregate structures has been unclear, [7] in animal studies, after a suspension of MSU crystals were injected into rabbits’ knees, a direct correlation between MSU crystals and aggregates was observed [8]. To our knowledge, there have been no studies to evaluate a threshold effect of MSU crystal concentrations and detection of such MSU aggregates on ultrasound.

As such, the aim of this study was to better understand the threshold of detection of aggregate findings on ultrasound and to correlate such findings with corresponding CPLM images in an in vitro study.

## 2. Materials and Methods

### 2.1. Sample Preparation

Patient-derived MSU crystal dense suspensions (liquid tophi) were obtained from 2 separate patients during routine clinical care. During the surgical resection of a tophus (from an olecranon bursa), the surrounding “gout milk” was obtained for the research team. From a separate patient with an acute gout attack of the knee, the synovial milk-like fluid provided the second source of MSU crystals.

All specimens were collected as part of routine clinical care. Excess samples not needed for clinical care, destined to be discarded, were instead de-identified and transferred to the senior investigator under a written protocol between the Department of Pathology and the senior investigator. This protocol was reviewed by the university IRB and deemed to be non-human subject research.

Separately, we prepared fabricated in-house synthetic crystals by dissolving 6.1 mL of 1 M sodium hydroxide (Sigma Aldrich—SA 72082, St. Louis, MO, USA) in 200 mL of sterile-filtered endotoxin-free water (SA W3500) and then heated to the boiling point. One gram of uric acid (SA U0881) was subsequently added, and the temperature was lowered to 60 °C. The pH was adjusted to 8.9, and the solution was left stirring for 4–5 h at room temperature. After cooling and stirring overnight in a cold room, the crystals were washed, recovered by filtration, and dried. Previous studies have demonstrated that these synthetic MSU crystals have a morphology similar (in size and shape) to crystals retrieved from patients with gout [9].

For diluent, we used synovial fluid derived from 1 of 2 patients with knee osteoarthritis (after confirming that each synovial fluid was free of crystals through a 5 min CPLM review of >30 high power fields by the senior investigator).

To the dry fabricated in-house crystals, we suspended 250 µg of crystals in 500 µL of synovial fluid to create a thick paste. Then, to each fabricated or patient-derived crystal suspension, we created up to 10 serial dilutions mixing even volumes of the crystal suspensions with crystal free synovial fluid in Eppendorf tubes.

### 2.2. Ultrasound & CPLM Imaging

For each MSU suspension, the Eppendorf tubes were immersed in ultrasound gel and scanned using a General Electric Logiq E9 (GE HealthCare, Chicago, IL, USA) ultrasound machine with a hockey stick probe (Figure 1). Settings ranging from 9 to 15 MHz frequency were adjusted to optimize the image quality depending on density of the crystal suspension. The US images have been rotated 90 degrees and cropped so that the Eppendorf tube images are vertical in Figure 1 (right side of image is closest to the probe, left side is farthest). The 100× CPLM images were obtained for each sample using Olympus BX43 CPLM (Olympus Corporation, Tokyo, Japan) with polarizer kit.



**Figure 1.** Urate suspension in Eppendorf on bed of ultrasound gel for imaging.

To provide a more homogenous suspension, prior to US and CPLM imaging, each dilution was placed on a vortex mixer for 10 s, then sat for approximately 5 min (to allow any microbubbles formed in the mixing process to dissolve back into solution). Longer standing (greater risk of settling) times were favored to minimize microbubble artifacts.

### 3. Results

Serial dilutions are presented in Figure 2. We used CPLM images to align Eppendorf tubes of similar crystal concentrations across the two patient-derived and one fabricated crystal suspensions. The starting crystal concentration for the olecranon bursa aspirate was approximately four times more concentrated than the suspensions from either the knee aspirate or fabricated crystals.

		Dilutions	None	1:1	1:2	1:4	1:8	1:16	1:32	1:64	1:128	1:256	Control
Panel A: Aspirate from Olecranon Bursa	Ultrasound												
	CPLM 100x												
Panel B: Aspirate from Knee Effusion	Ultrasound		No corresponding sample with similar concentration as Panel A										
	CPLM 100x		No corresponding sample with similar concentration as Panel A										
Panel C: Suspension of Fabricated Crystals in Synovial Fluid	Ultrasound Synthetic crystals		No corresponding sample with similar concentration as Panel A										
	CPLM 100x		No corresponding sample with similar concentration as Panel A										

**Figure 2.** Ultrasound and Compensated Polarized Light Microscopic (CPLM) images from patient derived and in-house fabricated crystal suspensions. Panel A—Ultrasound and Compensated Polarized Light Microscope (CPLM) images from serial dilutions of the thick milky fluid collected from the olecranon bursa at the time of surgical resection of a large tophus. Panel B—Ultrasound and CPLM images from similar serial dilutions of thick milky fluid collected from aspirate of an acute gouty knee flare and effusion. Panel C—Ultrasound and CPLM images of serial dilutions of in-house derived synthetic crystals.

For the olecranon bursa aspirate, the density of aggregates began to diminish at 1:8 dilution, significantly by 1:64 and was indistinguishable from crystal free synovial fluid for dilutions  $\geq$  1:128 dilutions. The corresponding CPLM showed aggregates of MSU crystals through 1:16 dilutions. MSU crystals without aggregates could still be seen on CPLM down to 1:512 dilutions.

For the less dense knee aspirate, a similar pattern of aggregate detection was seen the first four dilutions. The final three dilutions were indistinguishable from each other and from synovial fluid control.

The fabricated MSU crystals were not detected as aggregates either by US or CPLM. The synthetic synovial dilutions had a more homogenous hyperechoic appearance without the appearance of aggregates on US. Numerous synthetic crystals were also seen without any packing or clustering.

For the crystal free control fluid and the most dilute suspensions, faint hyperechoic sonographic flecks are noted. These echogenic flecks are infrequent and less intense than aggregates detected in the more concentrated samples and may represent residual microbubbles.

#### 4. Discussion

While detection of synovial fluid MSU crystals is diagnostic of gout, the aspiration of smaller joints is technically difficult, painful and performed less frequently in primary care offices [10]. US offers imaging capable of detecting MSU crystal deposits in joints and periarticular regions. The double contour sign and hyperechoic aggregates are the most common findings on the sonography of joints affected by MSU crystal deposition [11]. Our study demonstrates an association between presence US aggregates and the density of MSU crystals in synovial fluid analysis by CPLM examination.

Animal studies demonstrate that synovial-based MSU clusters correlate with US aggregates. These synovial crystal clusters were capable of inducing strong inflammatory reactions as noted on the histology and presence of power doppler ultrasound (PDUS) in regions of US aggregates [8]. Schauer [12] reported that MSU crystals induce the aggregation of neutrophil extracellular traps (NETs) within 10 min *in vitro*. When neutrophils are at high cell densities, the MSU-induced NETs form dense aggregates to sequester and degrade the pro-inflammatory mediators. Intraperitoneal injection of MSU crystals into mice treated with thioglycate, to induce neutrophil accumulation, resulted in aggregated MSU crystals. Furthermore, MSU crystals were found to promote such aggregation in a dose-dependent manner [12]. The more concentrated patient-derived dilutions, under CPLM in our study, frequently noted tightly packed MSU crystal aggregations. (See Figure 1, Olecranon CPLM panels 1:1, 1:2, and 1:8; Knee aspirate original sample and 1:1 through 1:4). Despite similar MSU crystal density, the fabricated crystals were not detected as aggregates on US or crystal packing under CPLM as observed from the patient-derived samples. These differences may reflect that synthetic suspensions lack other factors that contribute to crystal clumping (such as NETosis or fibrous structures that would be found in solid tophi) [13,14].

The limitations to our study include sampling error as the fluid in the Eppendorf tubes does not mimic the exact environment in the synovium of the knee or olecranon bursa. We tried to minimize settling and uneven dispersion by agitating the suspensions prior to scanning, but MSU crystals and aggregates do settle. Microbubbles formed during the mixing process may not have fully dissolved despite mixing and could be misconstrued as aggregates on MSUS. To limit this potential artifact, we evaluated the microbubble resolution over time and favored longer standing (greater risk of settling) times to minimize microbubble artifacts.

As we did not seek a specific US threshold (e.g., X aggregates per  $\text{cm}^2$ ) and with an expected low reproducibility related to sampling error, we did not conduct tests to evaluate the reproducibility or intra- or inter-rater reliability of our methods.

US aggregates can be seen in patients with CPPD. Similarly dense CPPD crystal aspirates are exceedingly rare and often small in size [15]. We did not look at clinical aspirates from patients with CPPD, and therefore cannot comment on potential similarities or differences. However, other authors have commented that US aggregates of MSU crystals have a higher degree of variability in size, shape and echogenicity compared with those of CPP. CPP US aggregates tend to be more uniform [16]. Other US findings (such as the double contour finding) more reliably distinguish MSU from CPP deposition



by the anatomical location of the crystal deposition [17,18]. In a proof-of-concept study, Filippou et al. noted that CPP does not generate substantial acoustic shadowing unlike hydroxyapatite (HA) or MSU crystals, which attenuate US in proportion to the crystal concentration. HA and MSU crystals were seen to attenuate the US beam at greater crystal concentrations in turn generating acoustic shadowing, whereas CPP did not regardless of an increased concentration [19].

OMERACT recognized that US aggregates are non-specific and later changed the overarching principle in which aggregates can only be scored if other US features of gout such as the DCS and/or tophi are/have been present and are not located in a tophus [20].

However, in clinical cases where there is no definitive US evidence of gout (tophi or DCS) and synovial aspiration is desired, our data suggest that the clinician ought to target a joint with US aggregates given the correlation with higher concentrates of CPLM MSU deposition. Observations from our methodology were collected in vitro. We need to be cautious as these observations may not translate to naturally occurring synovial dilutions. An in vivo dilutional study would be neither practical nor replicate clinical experience. To evaluate clinical correlates of US aggregates, a clinical study would require comparison of hundreds of aspirations (with and without US aggregates) and subsequent correlation with CPLM detection of crystals.

With the greater focus on less invasive techniques to diagnose crystal induced arthritis, studies comparing varying detection modalities may add value on the certainty of US findings. For example, there have been comparison studies between MSUS and DECT [21–23]. Additionally, Spectral Photon-Counting Computed Tomography (SPCCT) has been able to show finer crystal details than DECT [24]. Studies comparing US and SPCCT or other imaging modalities may be beneficial to validating US findings of aggregates.

In summary, the findings of aggregates on US images in patients with gout argue for higher concentrations of MSU crystals. Where the diagnosis of gout has not already been established, finding US aggregates would prompt a suspicion of gout and identify a good candidate target joint for diagnostic aspiration.

**Author Contributions:** Conceptualization, J.D.F.; methodology, J.D.F.; formal analysis, E.L. and J.D.F.; resources, V.K.R.; data curation, A.R.C. and J.D.F.; writing—E.L. and J.D.F.; writing—review and editing, E.L., N.D., B.P., V.K.R. and J.D.F.; supervision, J.D.F.; project administration, A.R.C. and J.D.F. All authors have read and agreed to the published version of the manuscript.

**Funding:** This research received no external funding.

**Institutional Review Board Statement:** This protocol was reviewed by the university IRB and deemed to be non-human subject research. Samples derived from routine clinical care destined to be discarded, were instead de-identified and transferred to the senior investigator under a written protocol between the Department of Pathology and the senior investigator.

**Informed Consent Statement:** Not applicable.

**Data Availability Statement:** Data is contained within the article.

**Conflicts of Interest:** The authors declare no conflict of interest with the following exception. Nicola Dalbeth has received consulting fees or grants from AstraZeneca, Dyve Biosciences, Horizon, Amgen, Selecta, ArthroSi, JW Pharmaceutical Corporation, PK Med, PTC Therapeutics, and Protalix, outside the submitted work.

## References

1. Zhu, Y.; Pandya, B.J.; Choi, H.K. Prevalence of gout and hyperuricemia in the US general population: The National Health and Nutrition Examination Survey 2007–2008. *Arthritis Rheum.* **2011**, *63*, 3136–3141. [[CrossRef](#)] [[PubMed](#)]
2. Richette, P.; Doherty, M.; Pascual, E.; Barskova, V.; Becce, F.; Castaneda, J.; Coyfish, M.; Guillo, S.; Jansen, T.; Janssens, H.; et al. 2018 updated European League Against Rheumatism evidence-based recommendations for the diagnosis of gout. *Ann. Rheum. Dis.* **2020**, *79*, 31–38. [[CrossRef](#)] [[PubMed](#)]
3. Neogi, T.; Jansen, T.L.; Dalbeth, N.; Franssen, J.; Schumacher, H.R.; Berendsen, D.; Brown, M.; Choi, H.; Edwards, N.L.; Janssens, H.J.; et al. 2015 Gout Classification Criteria: An American College of Rheumatology/European League Against Rheumatism collaborative initiative. *Arthritis Rheumatol.* **2015**, *67*, 2557–2568. [[CrossRef](#)] [[PubMed](#)]

4. Terslev, L.; Gutierrez, M.; Schmidt, W.A.; Keen, H.I.; Filippucci, E.; Kane, D.; Thiele, R.; Kaeley, G.; Balint, P.; Mandl, P.; et al. Ultrasound as an Outcome Measure in Gout. A Validation Process by the OMERACT Ultrasound Working Group. *J. Rheumatol.* **2015**, *42*, 2177–2181. [[CrossRef](#)] [[PubMed](#)]
5. Cazenave, T.; Martire, V.; Reginato, A.M.; Gutierrez, M.; Waimann, C.A.; Pineda, C.; Rosa, J.E.; Ruta, S.; Sedano-Santiago, O.; Bertoli, A.M.; et al. Reliability of OMERACT ultrasound elementary lesions in gout: Results from a multicenter exercise. *Rheumatol. Int.* **2019**, *39*, 707–713. [[CrossRef](#)] [[PubMed](#)]
6. Chowalloor, P.V.; Keen, H.I. A systematic review of ultrasonography in gout and asymptomatic hyperuricaemia. *Ann. Rheum. Dis.* **2013**, *72*, 638–645. [[CrossRef](#)]
7. Martillo, M.A.; Nazzal, L.; Crittenden, D.B. The crystallization of monosodium urate. *Curr. Rheumatol. Rep.* **2014**, *16*, 400. [[CrossRef](#)]
8. Pineda, C.; Fuentes-Gómez, A.J.; Hernández-Díaz, C.; Zamudio-Cuevas, Y.; Fernández-Torres, J.; López-Macay, A.; Alba-Sánchez, I.; Camacho-Galindo, J.; Ventura, L.; Gómez-Quiróz, L.E.; et al. Animal model of acute gout reproduces the inflammatory and ultrasonographic joint changes of human gout. *Arthritis Res.* **2015**, *17*, 37. [[CrossRef](#)]
9. Denko, C.W.; Whitehouse, M.W. Experimental inflammation induced by naturally occurring microcrystalline calcium salts. *J. Rheumatol.* **1976**, *3*, 54–62.
10. Newberry, S.J.; FitzGerald, J.D.; Motala, A.; Booth, M.; Maglione, M.A.; Han, D.; Tariq, A.; O’Hanlon, C.E.; Shanman, R.; Dudley, W.; et al. Diagnosis of Gout: A Systematic Review in Support of an American College of Physicians Clinical Practice Guideline. *Ann. Intern. Med.* **2017**, *166*, 27–36. [[CrossRef](#)]
11. Zhu, L.; Zheng, S.; Wang, W.; Zhou, Q.; Wu, H. Combining Hyperechoic Aggregates and the Double-Contour Sign Increases the Sensitivity of Sonography for Detection of Monosodium Urate Deposits in Gout. *J. Ultrasound Med.* **2017**, *36*, 935–940. [[CrossRef](#)]
12. Schauer, C.; Janko, C.; Munoz, L.E.; Zhao, Y.; Kienhöfer, D.; Frey, B.; Lell, M.; Manger, B.; Rech, J.; Naschberger, E.; et al. Aggregated neutrophil extracellular traps limit inflammation by degrading cytokines and chemokines. *Nat. Med.* **2014**, *20*, 511–517. [[CrossRef](#)] [[PubMed](#)]
13. Pieterse, E.; Jeremic, I.; Czegley, C.; Weidner, D.; Biermann, M.H.; Veissi, S.; Maueröder, C.; Schauer, C.; Bilyy, R.; Dumych, T.; et al. Blood-borne phagocytes internalize urate microaggregates and prevent intravascular NETosis by urate crystals. *Sci. Rep.* **2016**, *6*, 38229. [[CrossRef](#)]
14. Chatfield, S.M.; Grebe, K.; Whitehead, L.W.; Rogers, K.L.; Nebl, T.; Murphy, J.M.; Wicks, I.P. Monosodium Urate Crystals Generate Nuclease-Resistant Neutrophil Extracellular Traps via a Distinct Molecular Pathway. *J. Immunol.* **2018**, *200*, 1802–1816. [[CrossRef](#)] [[PubMed](#)]
15. Zell, M.; Aung, T.; Kaldas, M.; Rosenthal, A.K.; Bai, B.; Liu, T.; Ozcan, A.; FitzGerald, J.D. Calcium pyrophosphate crystal size and characteristics. *Osteoarthritis Cartilage* **2021**, *3*, 100133. [[CrossRef](#)] [[PubMed](#)]
16. Filippucci, E.; Di Geso, L.; Grassi, W. Tips and tricks to recognize microcrystalline arthritis. *Rheumatology* **2012**, *51* (Suppl. 7), vii18–vii21. [[CrossRef](#)]
17. Grassi, W.; Meenagh, G.; Pascual, E.; Filippucci, E. “Crystal clear”-sonographic assessment of gout and calcium pyrophosphate deposition disease. *Semin. Arthritis Rheum.* **2006**, *36*, 197–202. [[CrossRef](#)] [[PubMed](#)]
18. Frediani, B.; Filippou, G.; Falsetti, P.; Lorenzini, S.; Baldi, F.; Acciai, C.; Siagkri, C.; Marotto, D.; Galeazzi, M.; Marcolongo, R. Diagnosis of calcium pyrophosphate dihydrate crystal deposition disease: Ultrasonographic criteria proposed. *Ann. Rheum. Dis.* **2005**, *64*, 638–640. [[CrossRef](#)]
19. Filippou, G.; Pacini, G.; Sirotti, S.; Zadory, M.; Carboni, D.; Damiani, A.; Fiorentini, E.; Cipolletta, E.; Filippucci, E.; Froehlich, J.M.; et al. Comparison of ultrasound attenuation by calcium pyrophosphate, hydroxyapatite and monosodium urate crystals: A proof-of-concept study. *Ann. Rheum. Dis.* **2022**, *81*, 1199–1201. [[CrossRef](#)]
20. Christiansen, S.N.; Filippou, G.; Scirè, C.A.; Balint, P.V.; Bruyn, G.A.; Dalbeth, N.; DeJaco, C.; Sedie, A.D.; Filippucci, E.; Hammer, H.B.; et al. Consensus-based semi-quantitative ultrasound scoring system for gout lesions: Results of an OMERACT Delphi process and web-reliability exercise. *Semin. Arthritis Rheum.* **2021**, *51*, 644–649. [[CrossRef](#)] [[PubMed](#)]
21. Ahn, S.J.; Zhang, D.; Levine, B.D.; Dalbeth, N.; Pool, B.; Ranganath, V.K.; Benhaim, P.; Nelson, S.D.; Hsieh, S.S.; FitzGerald, J.D. Limitations of dual-energy CT in the detection of monosodium urate deposition in dense liquid tophi and calcified tophi. *Skelet. Radiol.* **2021**, *50*, 1667–1675. [[CrossRef](#)] [[PubMed](#)]
22. Zell, M.; Zhang, D.; FitzGerald, J. Diagnostic advances in synovial fluid analysis and radiographic identification for crystalline arthritis. *Curr. Opin Rheumatol.* **2019**, *31*, 134–143. [[CrossRef](#)] [[PubMed](#)]
23. Ogdie, A.; Taylor, W.J.; Weatherall, M.; Fransen, J.; Jansen, T.L.; Neogi, T.; Schumacher, H.R.; Dalbeth, N. Imaging modalities for the classification of gout: Systematic literature review and meta-analysis. *Ann. Rheum. Dis.* **2015**, *74*, 1868–1874. [[CrossRef](#)] [[PubMed](#)]
24. Stamp, L.K.; Anderson, N.G.; Becce, F.; Rajeswari, M.; Polson, M.; Guyen, O.; Viry, A.; Choi, C.; Kirkbride, T.E.; Raja, A.Y. Clinical Utility of Multi-Energy Spectral Photon-Counting Computed Tomography in Crystal Arthritis. *Arthritis Rheumatol.* **2019**, *71*, 1158–1162. [[CrossRef](#)] [[PubMed](#)]

**Disclaimer/Publisher’s Note:** The statements, opinions and data contained in all publications are solely those of the individual author(s) and contributor(s) and not of MDPI and/or the editor(s). MDPI and/or the editor(s) disclaim responsibility for any injury to people or property resulting from any ideas, methods, instructions or products referred to in the content.